Isomerization of a Single Aspartyl Residue of Anti-Epidermal Growth Factor Receptor Immunoglobulin γ2 Antibody Highlights the Role Avidity Plays in Antibody Activity

Douglas S. Rehder,*,§ Dirk Chelius,§ Arnold McAuley,§ Thomas M. Dillon,§ Gang Xiao,§ Jill Crouse-Zeineddini,|| Louisa Vardanyan,|| Natalie Perico,§ Venkat Mukku,|| David N. Brems,§ Masazumi Matsumura,§ and Pavel V. Bondarenko*,§

Process and Product Development, Amgen, Inc., Thousand Oaks, California 91320

Received September 5, 2007; Revised Manuscript Received November 21, 2007

ABSTRACT: A new isoform of the light chain of a fully human monoclonal immunoglobulin γ2 (IgG2) antibody panitumumab against human epidermal growth factor receptor (EGFR) was generated by in vitro aging. The isoform was attributed to the isomerization of aspartate 92 located between phenylalanine 91 and histidine 93 residues in the antigen-binding region. The isomerization rate increased with increased temperature and decreased pH. A size-exclusion chromatography binding assay was used to show that one antibody molecule was able to bind two soluble extracellular EGFR molecules in solution, and isomerization of one or both Asp-92 residues deactivated one or both antigen-binding regions, respectively. In addition, isomerization of Asp-92 showed a decrease in in vitro potency as measured by a cell proliferation assay with a 32D cell line that expressed the full-length human EGFR. The data indicate that antibodies containing either one or two isomerized residues were not effective in inhibiting EGFR-mediated cell proliferation, and that two unmodified antigen binding regions were needed to achieve full efficacy. For comparison, the potency of an intact IgG1 antibody cetuximab against the same receptor was correlated with the bioactivity of its individual antigen-binding fragments. The intact IgG1 antibody with two antigen-binding fragments was also much more active in suppressing cell proliferation than the individual fragments, similar to the IgG2 results. These results indicated that avidity played a key role in the inhibition of cell proliferation by these antibodies against the human EGFR, suggesting that their mechanisms of action are similar.

The human epidermal growth factor (EGF)[1] receptor (EGFR) is a 170 kDa transmembrane glycoprotein, which includes a single chain polypeptide of 131.6 kDa and approximately 40 kDa of sugar moieties (*1*, *2*). The mature EGFR contains an extracellular ligand binding region (*3*), a transmembrane domain, and an intracellular tyrosine kinase domain similar to other receptors from the ErbB family (*4*). A number of ligands, including EGF and transforming growth factor α (TGFα), bind to the extracellular domain of EGFR (*5*). Upon binding of the ligand, EGFR dimerizes with either another EGFR to create a homodimer or with another member of the ErbB receptor family to create a heterodimer, leading to signal transduction into the cell (*4*−*7*). Normally, EGFR signaling is tightly regulated, and overexpression of this receptor is linked to carcinomas and other human cancers. Several anticancer antibodies against EGFR extracellular region are now being used and tested in the clinic (*8*−*12*). Understanding of the mechanism of EGFR signaling and antibody−EGFR interactions on the cell surface is a very important research objective in ongoing development of novel EGFR-suppressing anticancer antibody therapies (*13*, *14*) and was one of the goals of this study.

Deamidation of asparagine (Asn) and isomerization of aspartic acid (Asp) are nonenzymatic modifications that affect peptides and proteins (*15*−*18*). Degradation of both Asn and Asp residues leads to formation of a succinimide intermediate, which spontaneously hydrolyzes to isoAsp and Asp in a typical ratio of 3:1 in short peptides (*15*, *19*). The destabilization of Asn residues to form a succinimide intermediate and then an isoaspartate is accelerated at alkaline pH, whereas isomerization of Asp is optimal at pH 4−5 (*16*−*18*). Asp isomerization was also reported in the calcium-binding domains of calmodulin during in vitro aging without calcium at pH 7.4, 37 °C (*20*). The Asp residues in these domains were highly flexible in the absence of calcium, which explained their susceptibility to isomerization (*20*). Although Asp isomerization increases in mildly acidic buffers, these buffers have been actively utilized for formulation of proteins including antibodies, because other covalent modifications, such as deamidation, oxidation, and enzymatic cleavages, and physical changes in proteins, including dimer

* Corresponding authors. (P.V.B.) Amgen, Inc., One Amgen Center Dr., MS 8-1-C, Thousand Oaks, CA 91320; tel (805) 447-7215; fax 805-447-3259; e-mail pavel.bondarenko@amgen.com. (D.S.R.) Amgen, Inc., 1201 Amgen Court West, MS AW2/D2152, Seattle, WA 98119; tel (206) 265-7446; fax (206) 217-0492; e-mail drehder@amgen.com.

§ Department of Pharmaceutics.

|| Department of Global Cellular and Analytical Resources.

[1] Abbreviations: EGF, epidermal growth factor; EGFR, epidermal growth factor receptor; Asp, aspartate; isoAsp, isoaspartate; LC, light chain; isoLC, iso-light chain; HC, heavy chain; SE, size-exclusion; RP, reversed-phase; MS, mass spectrometry.

10.1021/bi7018223 CCC: $40.75
Published on Web 01/31/2008

formation and aggregation, tend to be minimized at pH 4−6 (*21*, *22*). The kinetics of Asn deamidation and Asp isomerization have been studied extensively and the data consistently show glycine and serine to be the most destabilizing amino acids in the +1 position (*15*, *18*, *20*, *23*−*25*). Among several −1 residues tested, the His-Asp sequence was identified as particularly labile (*24*). The kinetic mechanism of succinimide formation and its hydrolysis in proteins is more complex compared to small peptides, because it is influenced by the position of Asn and Asp within the secondary and tertiary structures (*20*, *26*−*30*).

Complementarity-determining regions (CDRs) are hypervariable regions located in the heavy chain (HC) and light chain (LC) of antibodies and are responsible for antigen binding. CDR residues are located in the loops connecting β strands of the immunoglobulin fold. CDR loops are flexible, accessible to the environment, and often susceptible to degradations including Asp isomerization (*31*−*34*). Incorporation of an extra carbon atom in the peptide backbone and reorientation of the side group during isomerization of Asp resulted in structural changes and a decrease in efficacy of therapeutic antibodies (*31*, *32*).

Previously, Edman sequencing was used to detect and identify isoAsp residues (*35*). Another approach for the identification was the use of bovine brain protein carboxylmethyltransferase, an enzyme that specifically methylates the isoAsp sites (*19*). More recently, Zhang et al. (*36*) showed that Asp-N protease does not cleave at the N-terminus of isoAsp and employed this finding to identify Asp isomerization. Analytical characterization including detection and quantitation of protein molecules containing isoAsp converted from Asp remains a challenging task, because this modification does not change the mass or the net charge of the molecules. Despite these challenges, intact antibody molecules containing isoAsp residues were separated from the wild-type molecules by ion exchange (*32*) and hydrophobic interaction (*34*) chromatographic techniques because of the structural changes associated with the isomerization. Peptide mapping provided a separation method for peptides containing Asp and isoAsp (*15*, *36*, *37*). The peptides with isoAsp possess the same mass but typically elute earlier than the peptides with Asp (*15*). Although peptide mapping is a powerful analytical technique, it is time-consuming and may itself cause degradations during sample preparation and analysis (*38*, *39*). In this study, peptide mapping was used in conjunction with a recently developed high-resolution reversed-phase high-performance liquid chromatography online with mass spectrometry (RP HPLC/MS) method for separation of modifications in the antibody HC and LC (*40*).

Size-exclusion high-performance liquid chromatography (SE-HPLC) has been widely used to monitor dimer and aggregate formation in antibody stability studies (*41*, *42*). The technique was also utilized in several reports for characterization of noncovalent antibody−antigen complexes (*43*−*45*). In this study, SE-HPLC was employed to study the effect of the modifications of an anti-EGFR on its binding affinity to soluble human EGFR, particularly isomerization of an Asp residue on the LC.

MATERIALS AND METHODS

Materials. The anti-EGFR IgG2κ human monoclonal antibody ABX-EGF, panitumumab (*11*, *46*), was produced in a mammalian cell line and purified by standard techniques (*47*). IgG2 samples were aged in 10 mM sodium acetate and 10 mM sodium phosphate buffer, pH 5.0−5.2, at 29 and 37 °C for several months and compared with a control sample stored at −70 °C. The extracellular domain of human EGFR was produced and purified at Amgen and consisted of 623 N-terminal residues of the mature human EGF receptor (residues 25−647 of the human EGFR precursor, gi|2811086|sp|P00533|EGFR_HUMAN). The six-histidine tag was added at the C-terminal Ala-623 to facilitate purification of the protein. The calculated molecular mass of the soluble EGFR was 69 614 Da. It contained 12 N-glycosylation sites, and the sugar moieties increased the apparent molecular mass. The soluble EGFR was produced in the 293T cell line, localized in conditioned medium, and purified. The apparent molecular mass of the soluble EGFR (105 kDa) was determined by migration on 4−20% SDS−PAGE in nonreducing buffer versus Invitrogen prestained standard. The purity of EGFR (95%) was determined by analysis of a 5 μg protein load on a Coomassie blue-stained gel. The total protein concentration (0.45 mg/mL) was determined by UV absorption at 280 nm, using a calculated extinction coefficient of $\epsilon_{280} = 58\,800\ M^{-1}\ cm^{-1}$ or 0.84 cm^{-1} for 1 mg/mL. The EGFR was stored at −80 °C before use. The anti-EGFR IgG1, cetuximab, monoclonal antibody C225 (*48*, *49*) was produced in a mammalian cell line and purified as described in ref *50*. Previously (*49*), cetuximab sequences were deposited in GenBank as light gi|66361250|pdb|1YY8|D and heavy chain gi|66361248|pdb|1YY8|B.

Reduction and Alkylation of the Antibody and RP-HPLC/MS Analysis of Light and Heavy Chains. The experimental procedures for preparation and analysis of reduced and alkylated antibody were previously described by Rehder et al. (*40*). Agilent Zorbax SB300 CN column with 3.5 μm particle size, 300 Å pore size, 50 × 1 mm, was used for the HPLC/MS analysis. Solvent A was 0.1% aqueous trifluoroacetic acid (TFA; J.T. Baker, Phillipsburg, NJ) and solvent B contained 80% *n*-propanol (Burdick & Jackson, Muskegon, MI), 10% acetonitrile (ACN; J.T. Baker), 9.9% water, with 0.1% TFA.

ESI-TOF Mass Spectrometry of Intact and Reduced Antibodies. On-line with the RP chromatography, mass spectrometry was performed on a LCT Premier time-of-flight (TOF) mass spectrometer equipped with an electrospray ionization (ESI) atmosphere−vacuum interface (Waters, Milford, MA). The mass spectrometer was set to run in a positive ion mode with a capillary voltage of 3200 V, sample cone at 100 V, *m*/*z* range of 1000−5000, and mass resolution of 5000. The instrument was tuned and calibrated by use of multiply charged ions of trypsinogen, which has a molecular mass of 23 981.0 Da (catalog number T1143, Sigma). The deconvolution of ESI mass spectra was performed with a MaxEnt1 algorithm, part of the MassLynx software from Waters. More details of the RP HPLC/MS method for analysis of intact and reduced antibodies can be found in refs *40*, *51*, and *52*.

Asp-N Digestion of Modified and Native Light Chain. The LC isoforms were subjected to Asp-N digest in order to identify the site of isomerization. The isomerized light chain (isoLC) and native LC separated in Figure 1 were collected after elution from the RP-HPLC column and digested with Asp-N protease. The two HPLC fractions were dried with a

Speed Vac concentrator and reconstituted in 200 μL of 100 mM phosphate at pH 6.9. The Asp-N enzyme (Roche Applied Science, Indianapolis, IN) was added at a 1:10 ratio and incubated for 6 h at 37 °C. The digest was quenched with the addition of 20% formic acid to a final concentration of 0.2% formic acid.

RP-HPLC Separation of Asp-N Peptides. Asp-N peptides were separated by RP-HPLC on an Agilent 1100 HPLC unit equipped with a UV detector, autosampler, micro flow cell, and temperature-controlled column compartment. A Polaris Ether column, 250 × 2 mm, packed with 3 μm particle size, 300 Å pore size C18 resin (Varian, Torrance, CA) was used for the peptide map separation. Solvent A was 0.1% TFA in water and solvent B contained 90% ACN, 9.015% water, and 0.085% TFA. Tryptic peptides were injected into the RP-HPLC column, which was then equilibrated with 100% solvent A. A linear gradient from 0% to 50% B ran over 205 min. The column flow rate was 200 μL/min and its temperature was maintained at 50 °C. A total of 20 μg of protein digest was injected onto the column. The column eluate was analyzed by the UV detector and then directed to an on-line ion trap mass spectrometer.

Ion-Trap Mass Spectrometry for Asp-N Peptide Maps. The mass spectrometric method for the analysis of the peptide maps was adopted from Chelius et al. (*39*). In summary, the HPLC was directly coupled to a Finnigan LCQ DECA ion-trap mass spectrometer (Thermo Electron, San Jose, CA) equipped with an electrospray ionization source. The spray voltage was 4.5 kV and the capillary temperature was 250 °C. The fragmentation mass spectra were obtained by use of ion-trap collision energies of 35%. The digestion products were identified via SEQUEST algorithm of BioWorks version 3.1 (Thermo Finnigan, San Jose, CA) and a mass analyzer, which was written in house (*53*).

SE-HPLC of Antibody−EGFR Complexes. SE-HPLC of soluble EGFR, anti-EGFR, and their complexes was performed on an Agilent 1100 capillary HPLC system equipped with a UV detector, autosampler set at 37 °C, a normal flow cell and an ambient temperature-controlled column compartment (Agilent, Palo Alto, CA). The isocratic-flow solvent was 100 mM NaH_2PO_4, 0.5 M NaCl, and 5% ethyl alcohol at pH 7.0. A Tosohaas TSK guard column SW_{XL}, 40 × 6 mm, and two Tosohaas G3000SW_{XL} TSK gel-filtration columns in series with a 5 μm particle size, 300 × 7.8 mm (Tosoh Bioscience LLC, Montgomeryville, PA), were used for the SE analysis. The columns were operated at 37 °C and a flow rate of 200 μL/min. Antibody−receptor complexes were formed by mixing and incubating the antibody and soluble EGFR in a pH 7.4 phosphate-buffered saline (PBS, Gibco, Invitrogen Corp.) solution at 37 °C for 30 min. Several antibody:receptor ratios were studied and are discussed in the sections below.

RP-HPLC/MS of SE-HPLC Fractions of the Antibody−EGFR Complexes. Each eluting SE-HPLC fraction of the antibody-soluble EGFR complexes was captured on a trap column from Micro-Tech Scientific Inc., Vista, CA, which was a Zorbax stable bond SB300 C8 35 × 2 mm column with 5 μm particle size, 300 Å pore size. The RP column was connected to the line of the SE-HPLC system between the UV detector and the waste line to capture protein fractions after they passed the UV detector of the SE system. The RP column was manually connected to the waste line for the duration of elution of the peak of interest. Several identical RP columns were used to capture proteins from several fractions eluting during a single SE-HPLC separation. RP-HPLC/MS analysis of the SE-HPLC fractions of the antibody−receptor complexes was performed on a second Agilent 1100 (capillary) HPLC system. The RP column with captured proteins was first washed with solvent A for 10 min at 100 μL/min to remove salt and then eluted with linear gradient from 21% to 50% solvent B. The trap column was then positioned in front of the Zorbax SB300 CN, 50 × 1 mm column, described above, for RP-HPLC/MS analysis. The solvents included water with 0.1% trifluoroacetic acid in solvent A and 90% *n*-propanol, 9.9% water, and 0.1% aqueous TFA in solvent B. The column temperature was maintained at 75 °C with a constant flow rate of 50 μL/min. The eluate from the two columns was analyzed by the UV detector and then directed to the on-line ESI-TOF mass spectrometer described above.

On-Column Reduction of SE-HPLC Fractions of EGFR and Anti-EGFR Followed by Reversed-Phase HPLC/MS. An eluting SE-HPLC protein fraction of interest was captured on the Zorbax C8 column 35 × 2 mm and washed with solvent A for 10 min at 100 μL/min to remove salt. Then the trap column was positioned in front of the Zorbax SB300 CN, 50 × 1 mm column. A 40 μL aliquot of 30 mg/mL TCEP [tris(2-carboxyethyl) phosphine hydrochloride] solution in 0.1% formic acid (pH 3) was injected and slowly pumped through the column with captured protein with a flow rate of 5 μL/min from pump A. The column was maintained at 75 °C. The rest of the method was the same as in the RP-HPLC analysis of reduced and alkylated antibodies described above and in ref *40*, except for the elution gradient, which was from 23% to 31% solvent B.

SE-HPLC MALS of Anti-EGF and EGFR. Multiangle light scattering (MALS) was performed on-line with the SE-HPLC, on a Dawn EOS, Wyatt QELS, and Optilab Rex in series (Wyatt Technology, Santa Barbara, CA).

Limited Proteolysis of IgG1 and Purification of Fab Fragments of IgG1. Previously described limited Lys-C proteolysis of human monoclonal IgG1 antibodies (*54*) was utilized in this study to generate Fab and Fc fragments. In brief, 0.4 mL of 2 mg/mL IgG1 was added to 3.6 mL of 0.1 M Tris-HCl (pH 7.5) and then the diluted sample was incubated with lysyl endopeptidase (Lys-C, Wako Pure Chemical Industries, Ltd., Richmond, VA) for 30 min at 37 °C at a protein:enzyme ratio of 1:400. Fab fragments were purified with an ImmunoPure Fab preparation kit (Pierce, Rockford, IL). First, a 3-mL aliquot of the limited Lys-C digest of IgG1 was applied to the protein A column after it had been equilibrated. Then, a 6-mL aliquot of the binding buffer (pH 8.0, 0.1% EDTA, provided in the kit) was applied to the column. During this step, Fc fragments remained captured by the column, while Fab fragments were eluted and collected for further analysis.

Cell Proliferation Assay. The murine interleukin 3 (mIL-3) dependent cell line 32D clone 3 (CRL-11346, ATCC, Manassas, VA), which normally does not express EGFR, was modified to express the full-length human EGFR (Genbank accession number X00588 for human mRNA for precursor of EGFR). This was accomplished by transfection of the cells with the human EGFR gene that had been subcloned into the vector pLJ, which also contains a

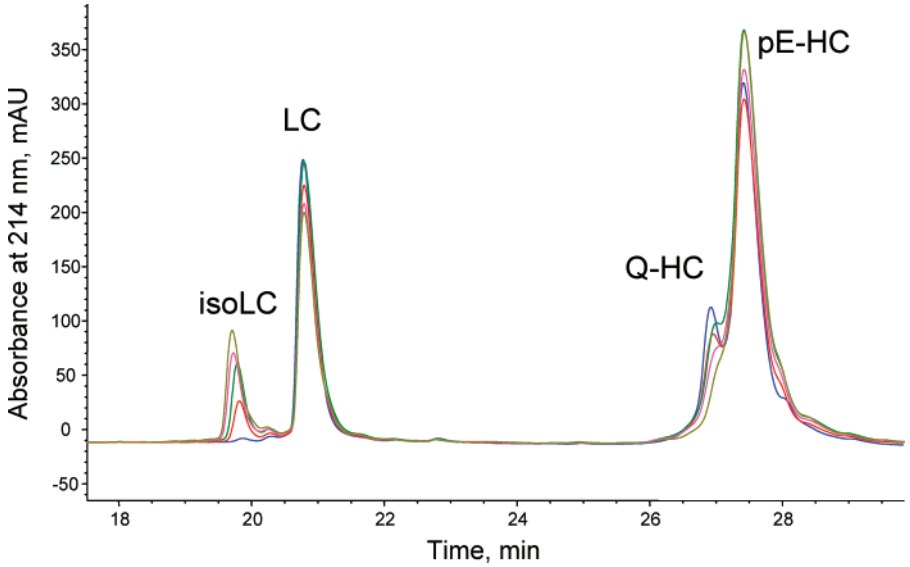

FIGURE 1: Reversed-phase chromatograms of reduced and alkylated anti-EGFR IgG2 antibody after aging in a pH 5.0 buffer. Blue indicates a control sample frozen at −70 °C. Other traces were from samples aged at 37 °C for 1, 2, 3, and 4 months. The modifications were identified as the isomerization of light chain (isoLC) and formation of pyroglutamic acid at the N-terminus of heavy chain (pE-HC).

neomycin (G418) resistance gene used as a selectable marker (*55*). Following transfection, a population expressing EGFR was enriched by staining the cells with an EGFR antibody followed by detection and sorting via flow cytometry. These cells responded to EGF and TGFα. This population was then transfected with a luciferase reporter gene under the control of an AP1 response element and SV40 promoter to facilitate reporter gene expression as an additional readout. However, in the experiments described in this paper, only cell proliferation readout was utilized. The cells were then grown in RPMI 1640 with GlutaMAX and HEPES (Invitrogen), 10% heat-inactivated fetal bovine serum (HyClone), Geneticin (Invitrogen), and 5 ng/mL recombinant mIL-3 (Amgen). For the assay, cells were washed with PBS and dispensed to Falcon 96-well clear plates at 20 000 cells/well. EGF ligand (R&D Systems) at a concentration of 0.85 ng/mL (0.15 nM) was incubated with control and aged anti-EGFR of varying concentrations. This concentration of the ligand was 70% of the saturation level. The samples were placed at 37 °C, 5% CO_2 in a humidified incubator for approximately 24 h. AlamarBlue (Accumed International), a redox dye that fluoresces in response to live cells, was added and the incubation was continued for an additional 24 h. Relative fluorescence was measured by use of a Fusion α (Perkin-Elmer) plate reader at 530 nm excitation, 590 nm emission. A four-parameter curve-fitting program was used to determine the inhibitory concentration (IC_{50}) of the antibody samples.

RESULTS

RP-HPLC/MS Analysis of Reduced and Alkylated Protein. RP-HPLC/MS analysis of the reduced and alkylated anti-EGFR after long-term aging at 29 and 37 °C in the mildly acidic buffers revealed two extra species in addition to the native LC and HC (Figure 1). The abundance of the pre-light chain peak eluting at 20 min increased under the specified aging conditions (10 mM acetate and 10 mM phosphate, pH 5, 37 °C) and reached 30% after 4 months (Figure 1) and 44% after longer storage. The deconvoluted ESI mass spectrum of the isoLC revealed a molecular mass value of 23 641 ± 0.5 Da, which was identical to that of the native LC (data not shown). Isomerization of Asp to isoAsp could result in a retention-time shift without changing the molecular mass, and it became the suspected chemical modification for earlier-eluting light-chain species. The HC was represented by two peaks, which were identified and characterized as earlier-eluting HC with N-terminal glutamine and later-eluting HC with N-terminal pyroglutamate (*40*). The percentage of remaining N-terminal glutamine decreased from approximately 30% to 15% after aging under the specified conditions (Figure 1).

Analysis of Asp-N Digests of the Light-Chain Variants. Asp-N peptide mapping of the collected LC variants revealed that the Asp-N protease cleaved at every Asp in the native LC fraction but was not able to cleave at Asp-92 of the variant LC fraction, identifying isomerization at this residue. The Asp-N peptide map of the isomerized light chain (isoLC) contained a peptide, D82F91isoD92S121, with missed cleavage at isoAsp-92 (isoD92, Figure 2A). The Asp-N digest of native LC contained separated peptides D82F91 and D92S121 with native Asp-92 (Figure 2B). All three peptides were identified by accurate mass measurements and MS/MS sequencing (Figure 3). The poor fragmentation in Figure 3A was attributed to the large size of the peptide and absence of a C-terminal basic residue as in tryptic or Lys-C peptides. In addition, rapid cleavages of D−H and F−P bonds produced strong b37 3+ and y29 2+ peaks and consumed the activation energy, leading to reduced intensities of other peaks and appearance of internal fragments. Despite the fact that the fragmentation mass spectra contained relatively few structural ions, the confidence of the peptide identification was high, because (1) the fragmentation pattern agreed with the two peptide fragments in Figure 3B,C and (2) the most abundant peaks in the fragmentation mass spectra occurred at the most likely cleavage sites according to ref *53* and other related studies. The Asp-N peptide maps strongly suggested that the earlier-eluting variant of LC was a modified LC with isomerization of Asp-92. The same results were obtained when a tryptic digestion method was performed on the samples, followed by Asp-N digestion of collected tryptic

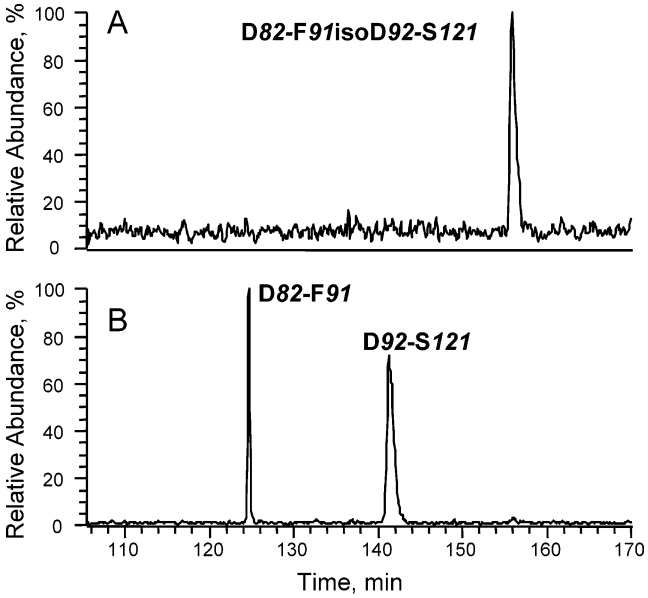

FIGURE 2: A section of reversed-phase selected ion chromatogram of Asp-N digest of iso-light chain (A) and native light chain (B) separated by reversed-phase chromatography of reduced IgG2 antibodies in Figure 1. Asp-N protease did not cleave at isoAsp residues, and this feature of Asp-N proteolysis was used to locate the site of isomerization. The peptides were identified by use of fragmentation mass spectra shown below. The base peak chromatograms were created from the most abundant ions of the three peptides: (1) D82IATYFCQHF91isoD92HLPLAFGGGTKVEIKRTVAAPSVFIFPPS121, *m*/*z* 1479, 3+; (2) D82IATYFCQHF91, *m*/*z* 651, 2+; and (3) D92HLPLAFGGGTKVEIKRTVAAPSVFIFPPS121, *m*/*z* 1051, 3+.

peptides containing Asp-92 and isoAsp-92 (data not shown). Racemization of L-Asp-92 to D-Asp-92 was another possibility that should be considered. Although racemization usually carries only a minor percentage in unstructured peptides and flexible sites (*15*, *56*), the succinimide racemization and subsequent hydrolysis can be directed to D-Asp formation in folded proteins.

Rate and Mechanism of IsoAsp Formation. The rate of Asp-92 isomerization increased with decreased pH. This observation was in agreement with the pH dependence of this reaction that has been reported in the literature (*16*). The isomerization of Asp-92 in the CDR3 of the LC was a very slow reaction during storage at 4 °C and pH 4.5−7.5. The percentage of isoLC increased only to 4% after 2 years of storage in mildly acidic buffers at 4 °C (data not shown). This indicated that although Asp isomerization is increased at pH 5.0 (*16*), the low temperature significantly slows this process. At pH 7.5 and 37 °C, Asp-92 was much more stable than in mildly acidic buffers (3% isoAsp after 3 months, data not shown), indicating that Asp-92 is stable under physiological conditions and is expected to be stable in a circulatory system. Isomerization of Asp is not kinetically favored at pH 7.5, unlike deamidation of Asn (*16*).

The pathway for isomerization of Asp involves formation of a succinimide intermediate followed by hydrolysis, resulting in isoAsp and Asp. In mildly acidic solutions, when the rate of cyclic imide formation was higher than the rate of its hydrolysis, accumulation of the succinimide intermediate was possible (*16*, *30*, *57*). To verify that isoAsp, rather than the succinimide intermediate, accumulated at LC residue 92 when aged in mildly acidic buffers, a rapid on-column

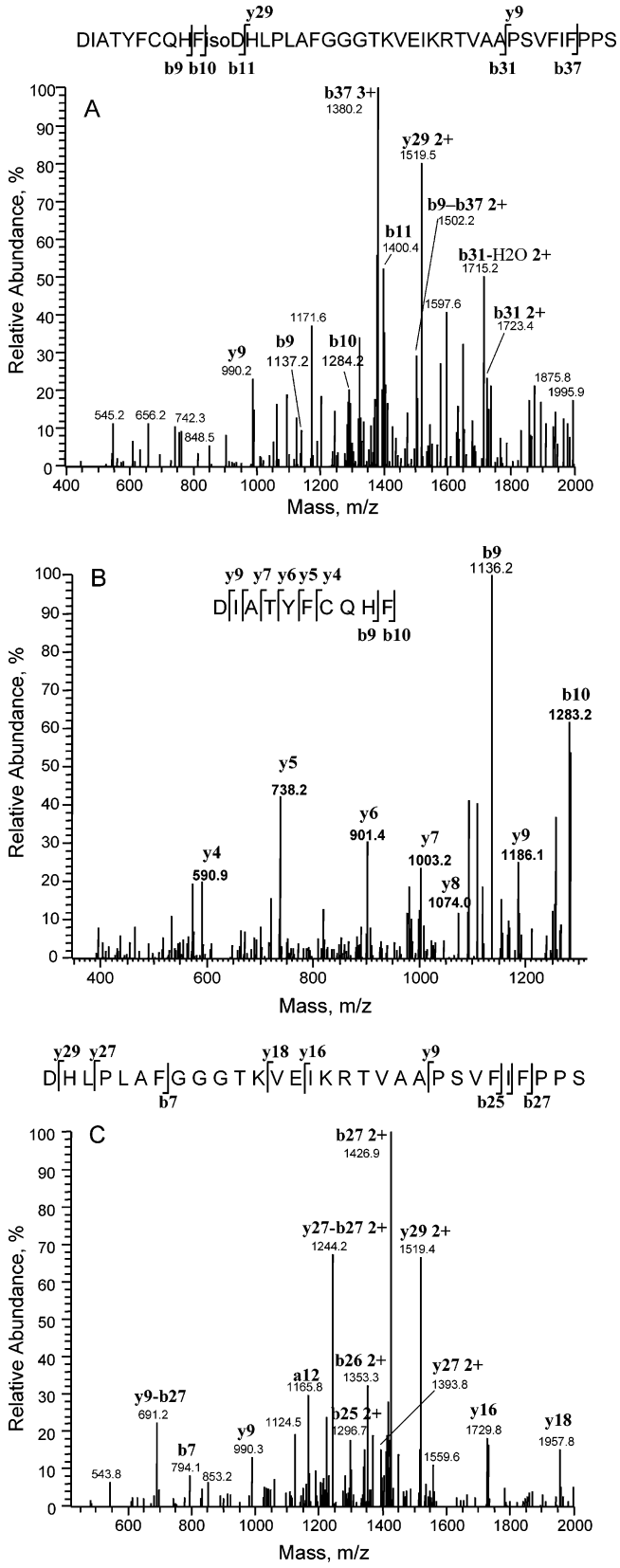

FIGURE 3: Fragmentation mass spectra of the peptides separated by reversed-phase chromatography of Asp-N digest of IgG2 in Figure 2: (A) D82IATYFCQHF91isoD92HLPLAFGGGTKVEIKRTVAAPSVFIFPPS121, *m*/*z* 1479, 3+ from iso light chain eluted at 156 min in Figure 2; (B) D82IATYFCQHF91, *m*/*z* 651, 2+ from native light chain eluted at 125 min; and (C) D92HLPLAFGGGTKVEIKRTVAAPSVFIFPPS121, *m*/*z* 1051, 3+ from native light chain eluted at 142 min. The tandem mass spectra confirmed identity of the peptides.

reduction in a low-pH solution (pH 3) was performed. During the sample preparation and analysis, the aged sample was not exposed to neutral pH. The antibodies unfolded and reduced at pH 3 and 7.5 (as described under Materials and Methods) showed equal percentage of isoLC and no succinimide intermediate as measured by RP-HPLC/ MS of reduced antibodies (data not shown). In addition, ^{18}O labeling of possible succinimide intermediates was performed by incubating the aged sample (and hydrolyzing the succinimides) in ^{18}O-water-containing buffer at pH 7.5 according to the previously described procedure (*30*). This analysis revealed a very small percentage (~6% ± 5%) of succinimide, confirming that the modification was indeed isoAsp-92 and not succinimide 92.

IgG2 Antibody−Receptor Binding Analysis by SE-HPLC. A SE-HPLC assay was developed to determine whether isoAsp-92 formation affected the antibody binding. Anti-EGFR and EGFR were injected separately to determine elution times and peak areas. The antibody and receptor were then mixed, incubated, and analyzed by the same SE-HPLC assay. The relative quantitative measurements were performed with detection at 214 nm, taking into account the following considerations. The peptide bond group dominates far-UV absorbance for proteins at 214 nm (*58*). Therefore, the protein absorbance at 214 nm is proportional to the number of peptide bonds and weight (in grams) of the protein portion. The numbers of peptide bonds were 1312 and 629 for anti-EGFR and EGFR, respectively. The ratio of the peptide bonds found in anti-EGFR and EGFR (2.09) was similar to the ratio of their molecular weight values (MW 144 037/69 614 = 2.07). The extracellular domain of EGFR was heavily glycosylated with approximately 35 kDa of oligosaccharides, which increased its molecular mass to approximately 105 kDa, although they remained "invisible" to the 214-nm light detector. The antibody (147 kDa) was also glycosylated with approximately 3 kDa of sugar moieties. The molar amount of receptor was 2 times greater than the molar amount of the antibody (Figure 4). Because the MW of the protein portion of EGFR is 2 times lower than for the antibody, their peak areas were approximately equal, as anticipated (Figure 4A−C). Although the EGFR had a smaller total molecular mass (105 kDa) as compared to the antibody (147 kDa), it eluted approximately at the same time (Figure 4C). This is most likely due to the glycosylation, which increased the hydrated volume of EGFR. Comparison of Figure 4 panels A and B shows that modifications of the anti-EGFR caused by aging did not change the peak area or SE-HPLC elution profile of the molecule, except for a minor loss most likely due to precipitation of the antibody sample after 8 months of storage at 37 °C (Figure 4B). For the SE-HPLC binding study (Figure 4D,E), the appearance of peaks eluting earlier than either the antibody or receptor was attributed to the formation of a high molecular weight complex composed of anti-EGFR and EGFR. The control antibody and EGFR formed a high molecular weight complex (SE1 in Figure 4), which consumed all monomer molecules and therefore contained antibody−receptor complexes at a ratio of 1:2. When the antibody and soluble EGFR were mixed in a 1:4 molar ratio, the peak area of the complex did not increase, but the monomeric, nonbound EGFR appeared at 78 min (data not shown). The native anti-EGFR bound only two receptors

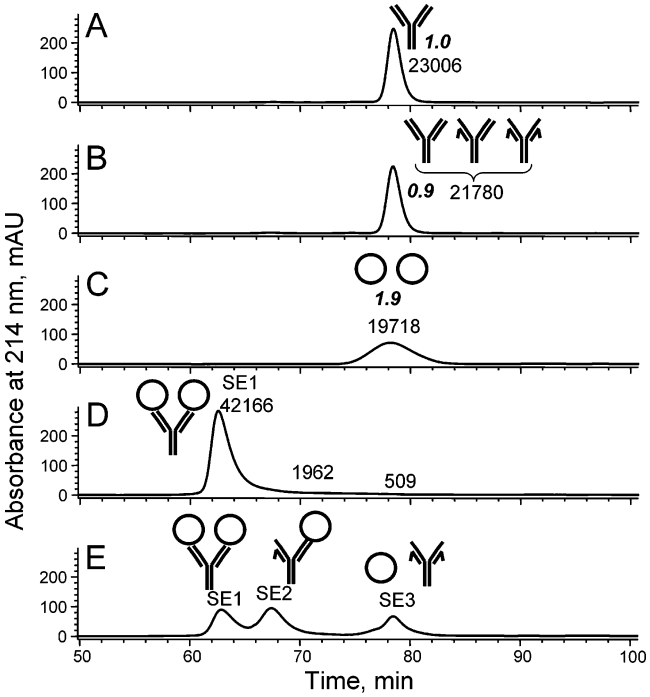

FIGURE 4: Size-exclusion chromatograms of the extracellular portion of human epidermal growth factor receptor (EGFR,○); anti-EGFR IgG2 antibody and their complexes. (A) Control sample of anti-EGFR stored at −70 °C; (B) sample of anti-EGFR aged to obtain 44% iso-light chain as measured by RP HPLC assay; (C) EGFR, a 105 kDa glycoprotein, including a single chain polypeptide of 70 kDa; (D) mixture of control IgG2 and EGFR at 1:2 molar ratio; (E) mixture of aged anti-EGFR and EGFR at 1:2 molar ratio. The peaks area for fractions SE1, SE2, and SE3 were 13 148, 17 543, and 11 630. The measured peak areas (in units of milliabsorbance units·second) are shown for each peak to prove that there was no significant protein loss in the experiments. The molar ratios in panels A−C (numbers in boldface italic type) were calculated by dividing the measured peak areas by the molecular weight of the protein portion on the molecules (MW 144 037 and 69 614 for anti-EGFR and EGFR, respectively) and normalizing to the control anti-EGFR.

even if the receptors were available in excess. The anti-EGFR was degraded to the extent of 44% of isoLC as measured by the RP-HPLC method for reduced antibody illustrated in Figure 1. The aged antibody did not bind as efficiently as the control antibody, resulting in an additional, smaller complex eluting at 67 min (SE2) and a fraction of unbound monomers eluting at 78 min (Figure 4E).

Identification and Quantitation of Intact Proteins from SE1, SE2, and SE3 fractions by RP-HPLC/MS and the Chains after On-Column Reduction. The proteins in fractions SE1, SE2, and SE3 were captured on three RP columns and then eluted to produce RP chromatograms shown in Figure 5 panels A−C, respectively. The RP chromatograms included the anti-EGFR IgG2 antibody that eluted at 13.5 min and EGFR that eluted at 19 min. The IgG2 antibody was identified by measuring the molecular mass value of 146 928 Da via the on-line ESI-TOF mass spectrometer. The soluble EGFR produced a very complex mass spectrum with multiple peaks (a broad bump between *m*/*z* 1500 and 4000) due to the multiple glycosylated forms of the protein, which could not be deconvoluted, but was sufficient to identify it as a heavily glycosylated protein. The RP elution times were confirmed by injecting the IgG2 antibody and soluble EGFR separately on one of the RP columns (data not shown).

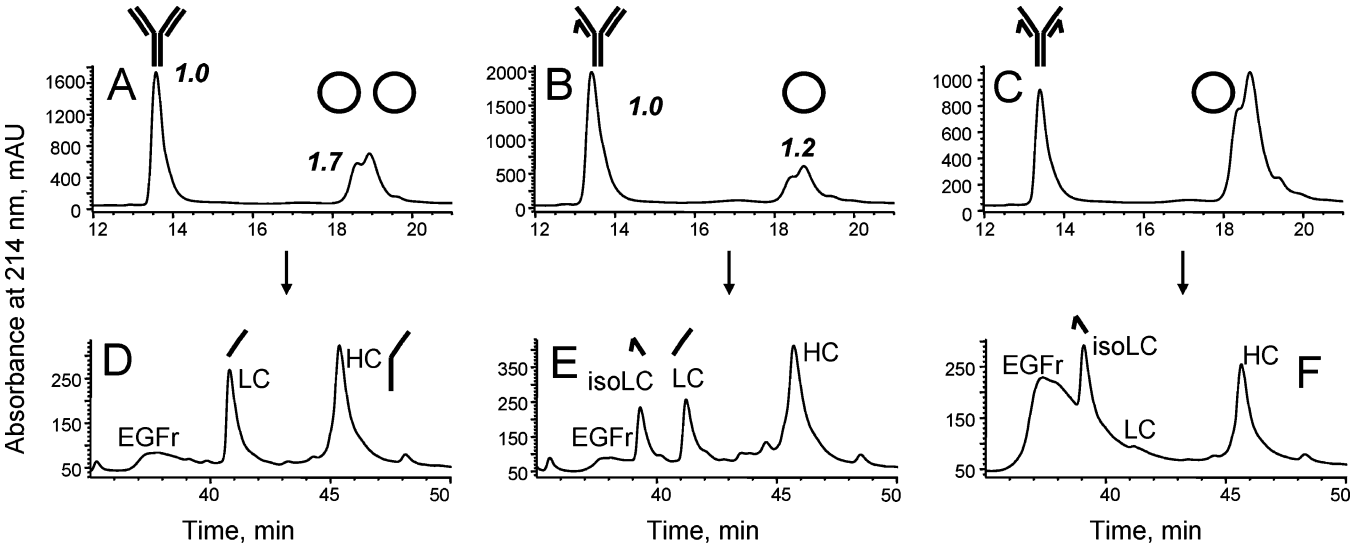

FIGURE 5: Identification of complexes between aged anti-EGFR IgG2 antibody and EGFR. Proteins from each eluting size-exclusion fraction were captured on a reversed-phase column, washed with 0.1% aqueous TFA, and eluted with organic solvent gradient for RP-HPLC/UV/MS analysis. (A−C) Reversed-phase chromatograms of size-exclusion fractions SE1, SE2, and SE3 from Figure 4, respectively. (D−F) Reversed-phase chromatograms of reduced size-exclusion fractions SE1, SE2, and SE3, correspondingly. The reduction was performed on column by injecting 30 mg/mL TCEP for 10 min before the RP-HPLC/UV/MS analysis. The molar ratios in A and B (numbers shown in boldface italic type) were calculated by dividing the peak areas by the molecular weight of the protein portion of the molecules (MW 144 037 and 69 614 for anti-EGF antibody and EGFR, respectively) and normalizing to the anti-EGF antibody.

According to the RP-HPLC/UV analysis, the SE1 fraction contained a 1:1.7 molar ratio of anti-EGFR to EGFR (Figure 5A). The molar ratio was calculated by dividing the peak areas by the corresponding MW for each species (MW 144 037 and 69 614) and normalizing to the peak area of IgG2 antibody. The protein ratio in fraction SE1 (eluting at 63 min from SE-HPLC) was close to 1:2, suggesting that one antibody was bound to two receptors in this SE fraction. The antibody:receptor ratio for SE1 was also derived from Figure 4D, where the antibody and receptor were mixed in a 1:2 molar ratio to produce a single SE peak of the antibody−receptor complex. The molar ratio of anti-EGFR to EGFR was 1.0:1.2 in fraction SE2 (Figure 5B), indicating that one antibody was bound to only one receptor in this fraction. The slight deviations from the even ratio numbers were caused probably by sample carryover during collection of partially separated SE fractions.

To assess the conformation of Asp-92 of the LC in each SE fraction, the captured proteins were reduced with TCEP directly on the RP columns followed by the organic gradient elution (Figure 5D−F). The on-column method of reduction was performed rather than conventional reduction in solution because the on-column method minimized losses otherwise seen during sample handling. The proteins were denatured in the hot (75 °C), low-pH (pH 2−3) environment of the RP column and then reduced during the 8 min of passage of the TCEP solution through the column with captured protein. As a result, the antibody was denatured and reduced on-column to produce LC and HC. The analyzed SE1 fraction contained only the native LC, SE2 included both isoLC and LC in approximately equal proportions, and SE3 contained only the isoLC (Figure 5D−F). This result indicated that native LC is required for binding to EGFR. Isomerization of the Asp-92 residues in one or both antigen-binding regions reduced the number of bound receptors to 1 or 0, respectively. The quantitative measurements and antibody−antigen ratios measured at 214 nm agreed with the measurements at 280 nm (data not shown).

Molecular Mass Measurements of Protein Complexes in SE1, SE2, and SE3 Fractions by MALS. Although Figures 4 and 5 indicated that the complexes contained antibody and receptor molecules at a ratio of approximately 1:2 for the control IgG2 antibody and 1:1 for the antibody molecules with one Asp-92 and one isoAsp-92, it was not clear if one native IgG2 antibody was bound to two receptors or if two antibodies were bound to four receptors in a complex. To determine the binding ratio in the complexes, molecular mass values of the antibody−EGFR complexes and the monomers were determined via the multiangle light scattering (MALS) detector coupled to the SE-HPLC. The measured molecular mass value of SE1 complex, 400 kDa, agreed with the combined molecular mass of antibody and two molecules of EGFR, 357 kDa [147 + (105 × 2) = 357]. The measured molecular mass value of SE2 complex, 280 kDa, was approximately equal to one antibody and one EGFR, 252 kDa (147 + 105 = 252). Finally, the measured molecular mass value of SE3 (170 kDa) was approximately equal to the molecular mass values of antibody and EGFR. All measured values were systematically higher than calculated values, probably because EGFR appears larger in size than it is, as it did in the SE measurement (Figure 4C).

Cell Proliferation Assay of IgG2 with Modified and Native Light Chain. Murine interleukin 3 (mIL-3) dependent 32D cells are murine hematopoietic progenitors that lack endogenous ErbB receptors and ligands (*59*). These cells have been used previously to study EGFR signaling and its inhibition by tyrosine kinase inhibitors and cetuximab IgG1 antibody (ref *60* and referenced in it articles). It was shown that the 32D EGFR cells express all of the intracellular components of the EGF signaling pathway necessary to induce a mitogenic and proliferation response (*59*), including Cbl- and AKT-mediated cascades (*60*, *61*).

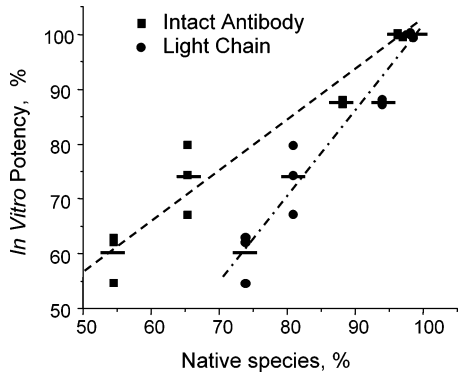

FIGURE 6: Correlation between in vitro bioactivity and percentage of native LC and native intact anti-EGFR IgG2 antibody aged in a pH 5 buffer. Percentage of native light chain was measured by the reversed-phase chromatography assay shown in Figure 1. The percentage of the native antibody was linked to the percentage of native light chains by the equation $Ab = LC^2$. In vitro bioactivity was measured by the cell proliferation assay. The bioactivity decreased with decreasing amount of remaining native light chain according to a fitted linear regression trend line $y = 1.50x - 50$ with $R^2 = 0.97$. For the calculated abundance of intact antibodies, a linear regression trend line was fitted to the equation $y = 0.83x + 17$ with $R^2 = 0.98$.

The two light chains of an IgG antibody are located in different antigen-binding fragments (Fab) separated by a flexible hinge, preventing the Fabs from interacting with each other. Therefore, modification events on the different Fab regions of the same intact molecule are statistically independent and the probability of occurrence of an intact unmodified antibody molecule can be described as $Ab = LC^2$, where LC is the fraction of unmodified light chain. This information was used to establish a correlation between the bioactivity, as measured by the 32D EGFR cell proliferation assay, and the percentage of unmodified LC and intact antibody for the aged sample (Figure 6). The percentages of native LC and native intact antibody (Figure 6) were measured from the RP chromatogram in Figure 1 for LC and derived from the statistical considerations ($Ab = LC^2$) for native intact antibody, respectively. The linear trend for the native LC shows a large negative intercept, suggesting the relationship between the potency and the percentage of native LC is not linear. The large positive slope indicated that potency decreased more rapidly than the percentage of native LCs. The linear regression of the intact antibodies had a positive intercept (17%) and a slope of nearly 1 (0.83), suggesting that the bioactivity of antibodies with one native and one isoLC is significantly less than for antibodies with both native LCs. In addition, a slope of near 1 indicated that the data showed a direct correlation between the percentage of remaining intact native antibodies (but not native LCs) and their bioactivity. To conclude, the biological activity assay indicated that isomerization of at least one LC deactivated the entire antibody molecule, hence avidity (binding with both antigen-binding regions) is an important feature of the anti-EGFR binding to the EGFR on the cell surface. Separating the antibody variants and subjecting them to the bioassay would provide a more quantitative measurement of the avidity affect. Thus far, only the receptor-assisted SE-HPLC method was capable of separating the Asp-92 antibody variants. However, because these fractions contained the antibodies bound to the soluble receptor, they are not suitable for the bioassay.

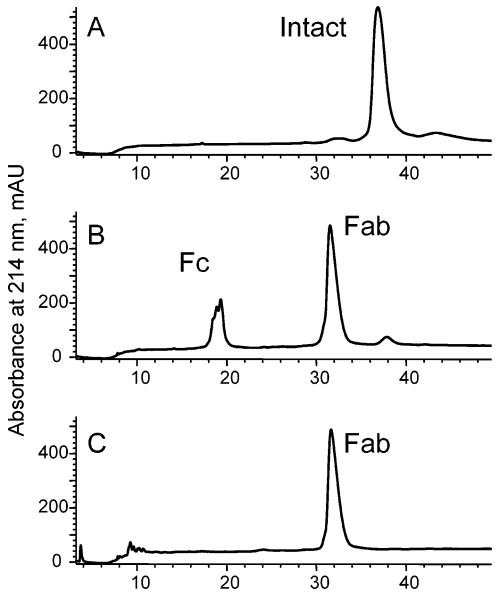

FIGURE 7: Reversed-phase chromatograms of IgG1: (A) as intact molecule; (B) Fab and Fc fragments after limited proteolysis with Lys-C protease, and (C) Fab fragments only after limited proteolysis and protein A column purification, which removed Fc.

Cell Proliferation Assay for IgG2, IgG1, and Fab Fragments of IgG1. In addition to the IgG2 molecule, an anti-EGFR IgG1 (C225, cetuximab) was used to compare potency of bivalent intact IgG1 and monovalent Fab fragments in inhibiting 32D EGFR cell proliferation in a classical setting for avidity study (intact versus Fab), analogous to the investigations with A431 cells (*62*, *63*). A second goal of using IgG1 was to directly compare these two anti-EGFR molecules, cetuximab and panitumumab, in the same assay. Biological potency of the intact bivalent IgG1 antibody with two Fab domains was compared to the potency of individual Fab fragments. In previous studies, the Fab fragments of 225 were obtained by pepsin cleavage below the hinge, followed by reduction of hinge disulfides with L-cysteine and alkylation with iodoacetamide (*62*) according to the early protocols (*64*, *65*). In this study, the fragments were produced by limited Lys-C proteolysis of IgG1 (C225), which cleaved between Lys-222 and Thr-223 (EU nomenclature) above the hinge. The Lys-C proteolysis was found to be an effective and simple method for producing the Fab fragments of human IgG1, because it did not require reduction and alkylation (*54*). At this time, we have not been successful in obtaining useful yields of Fab fragments from human IgG2 by either pepsin or Lys-C cleavage methods. Human IgG2s have a shorter and less accessible hinge, thereby restricting its cleavage by these enzymes. Hence, we used the Asp-92 isomerization as the means for producing monovalent IgG2 antibodies with only one binding Fab. Limited proteolysis of IgG1 and protein A purification of Fab fragments were monitored by RP HPLC/UV/MS analysis (Figure 7). The mass spectra were used to confirm the masses of fragments and ensure that there were no other cleavages (data not shown). This was important for the interpretation of the cell proliferation results. The resulting solution of purified Fab fragments had the same molar concentration of Fab fragments as the solution of intact IgG1 antibody. The IgG2, IgG1, and Fab IgG1 fragments were all tested in the same cell proliferation assay with the same cell preparation. The results,

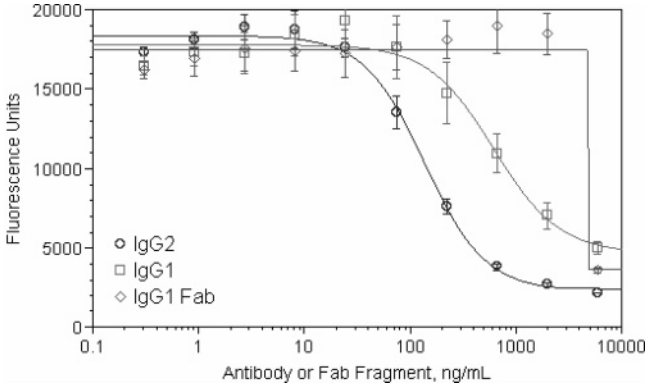

FIGURE 8: Inhibition of EGF-induced cell proliferation by bivalent IgG2 and bivalent and monovalent IgG1 against EGFR. The murine interleukin 3 (mIL-3) dependent cell line 32D clone 3 was modified to express the full-length human EGFR. The cells were grown with 0.85 ng/mL (0.15 nM) exogenous EGF and varying concentrations of bivalent IgG2 (○), bivalent IgG1 (□), and purified Fab fragments of IgG1 (◇). The error bars represent the standard deviation after three measurements ($n = 3$).

illustrated in Figure 8, show IC_{50} values of 0.9 nM (140 ng/mL) for IgG2, 4.1 nM (620 ng/mL) for IgG1, and approximately 25−80 nM (∼2000−4000 ng/mL) for the isolated Fab fragments (Figure 8). Therefore, a pair of Fab fragments was approximately 3−10 times less active than one intact IgG1 molecule. The dose−response curve for the Fab fragments was atypical, and therefore the IC_{50} value is only approximate. The data indicate that one Fab fragment was at least 7 times less active than the bivalent intact IgG1. Our results were in agreement with previous studies using a murine predecessor of cetuximab IgG1 antibody, which revealed that monovalent 225 Fab had weaker inhibition effects on the proliferation of several cell lines (*62*). To conclude, bivalent binding by both IgG1 and IgG2 increased the efficacy of both antibodies with respect to the related monovalent species. IgG2 was approximately 5 times more potent than the IgG1 in inhibiting proliferation of the 32D EGFR cells.

Competitive SE-HPLC Binding Assay of IgG2 and IgG1. SE-HPLC was used to compare the strength of the monovalent binding of the two IgG molecules and establish if they will compete for the same binding site. The individual proteins as well as their mixture at 1:1:2 ratio of IgG2/IgG1/EGFR were analyzed by SE-HPLC (Figure 9). Earlier SE-HPLC studies showed that each IgG2 antibody bound two receptors in solution (Figure 4). The same result was obtained for the IgG1 antibody (data not shown). In the IgG2/IgG1/EGFR mixture, the antibodies had to compete for the receptor, which was in deficit. In the SE-HPLC assay, the antibody−EGFR complexes eluted at 63 min, while unbound monomeric antibodies eluted at 77 min (Figure 9D). The elution time of the unbound monomer agreed with that of IgG1, which elutes slightly earlier than IgG2 (Figure 9A,D). To further confirm the identities of the bound and unbound species, the complex and the monomer were captured on RP columns maintained at 75 °C and eluted with an organic gradient of increasing *n*-propanol at pH 2. The high-temperature and low-pH conditions of the reversed-phase chromatography created a denaturing environment that allowed for the dissociation and separation of the individual components of the complex (Figure 10A,B). In turn, on-line identification by mass spectrometry of each component was

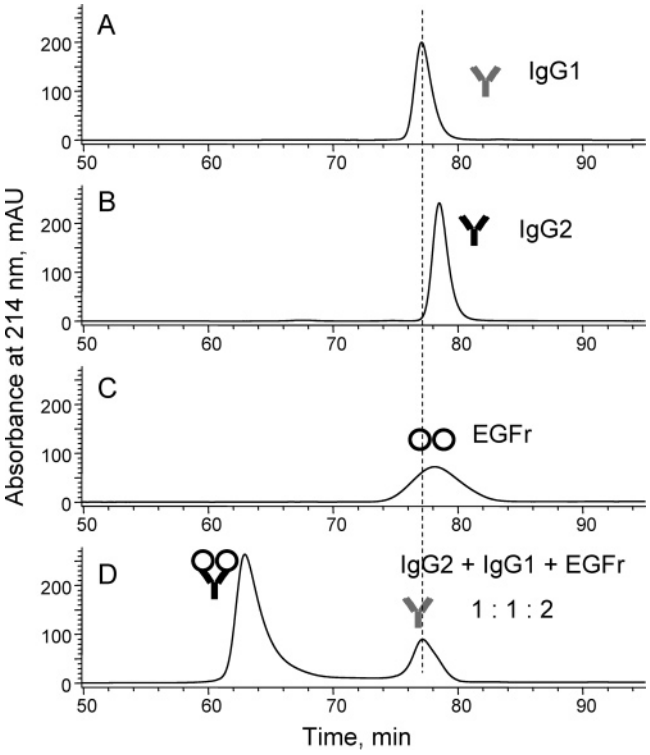

FIGURE 9: Size-exclusion competitive binding HPLC assay. Size-exclusion chromatograms of IgG2 (A), IgG1 (B), EGFR (C), and the mixture of IgG2/IgG1/EGFR at 1:1:2 ratio (D) are shown.

made feasible (Figure 10C−E). IgG1 produced a larger mass and a broader glycosylation profile compared to IgG2, consistent with the extra N-glycosylation in the Fab region of IgG1 (Figure 10E). The *m*/*z* mass spectrum of EGFR contained a broad distribution of multiple peaks, which could not be deconvoluted and which was indicative of a heavily glycosylated protein (Figure 10D). The IgG2 and IgG1 molecules were sufficiently separated by the RP method to conclude that the complex mainly contained IgG2 and EGFR and the unbound fraction was mainly due to IgG1 (Figure 10A,B). The IgG2:IgG1 peak area ratio was approximately 5:1 for the antibodies bound to the receptor and 1:5 for the antibodies that did not bind to the receptor (Figure 10A,B).

DISCUSSION

These experiments compared efficiency of bivalent and monovalent species of two anti-EGFR antibodies, panitumumab IgG2 and cetuximab IgG1, to inhibit proliferation of 32D EGFR cells. In the case of IgG1, a conventional approach was utilized by comparing potency of bivalent intact IgG1 and monovalent antigen-binding fragment (Fab) produced by limited proteolysis of IgG1. Human IgG2 have a shorter and less accessible hinge, restricting cleavage by pepsin or Lys-C proteases. In this report, a unique property of IgG2, isomerization of the light chain Asp-92 in mildly acidic buffers at elevated temperatures, was explored to disable one Fab region and obtain a monovalent IgG2 antibody. Of the 31 Asp residues in the IgG2, only Asp-92 underwent significant isomerization. Crystal structures of available IgG antibodies (*66*) indicated that Asp-92 (EU numbering) was located in a flexible region (CDR3) exposed to solvents, unlike the other Asp residues located in folded regions. Asp-92 was followed by histidine (His), indicating

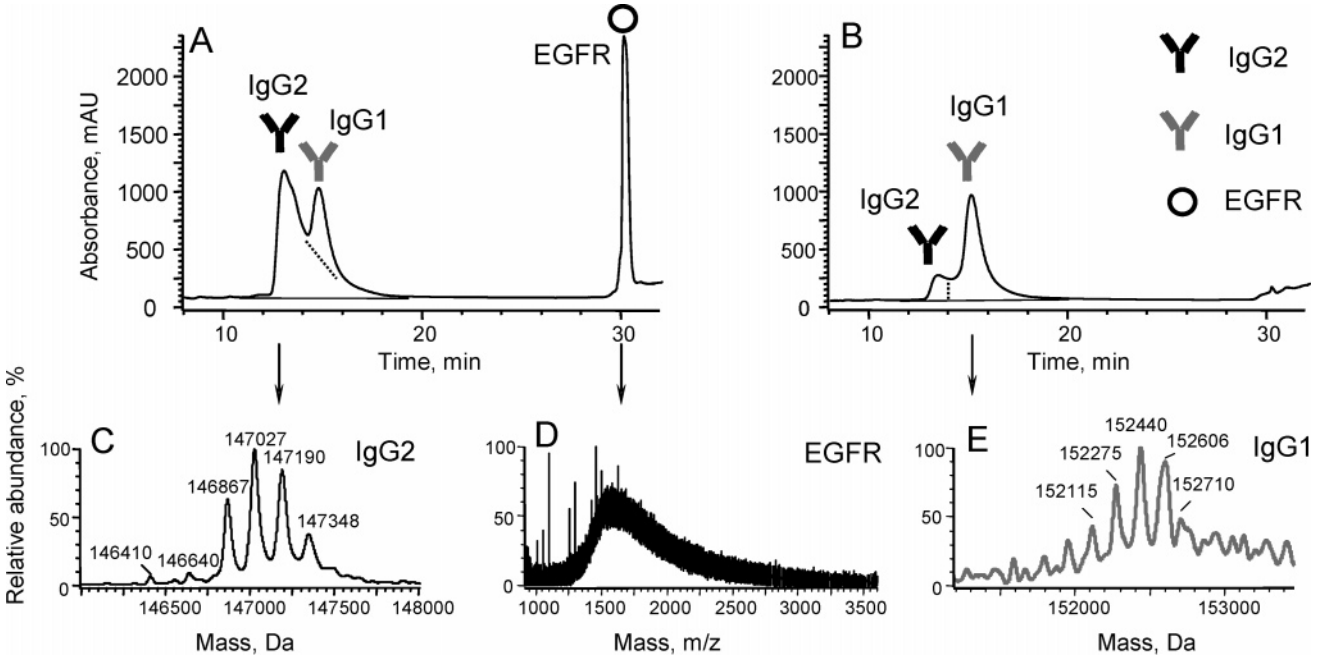

FIGURE 10: Identification of complexes produced by the IgG2/IgG1/EGFR mixture at 1:1:2 ratio and separated by size-exclusion chromatography in Figure 9D. The fractions containing the antibody-EGFR complex eluting at 63 min and monomeric species eluting at 77 min (Figure 9) were captured on two reversed-phase columns. (A, B) RP chromatograms of the antibody−EGFR complex and the monomers, respectively, eluted from the reversed-phase column. (C−E) Deconvoluted ESI mass spectra of IgG2 with molecular mass 147.8 kDa and heavily glycosylated EGFR and IgG with molecular mass 152.1 kDa, respectively.

that His at the +1 position created a destabilizing motif in this molecule, contrary to the previous observations for short peptides (*24*). Upon aging in mildly acidic buffers, a population of the intact monovalent anti-EGFRs was produced with one Fab region inactivated by isomerization of Asp-92 residue in the receptor-binding domain.

Bivalent binding by IgG1 or IgG2 increased the efficacy of the intact antibodies with respect to the related monovalent species in inhibiting proliferation of 32D EGFR cells. This was probably due to increased cell surface affinity of the bivalent antibodies facilitated by the avidity. In a study by Fan et al. (*63*) of the murine version of intact IgG1 (225) and 225 Fab fragments, the rate of dissociation from the A431 cell surface was at least 5 times lower for the intact antibody compare to Fab. The cell surface retention time decreased from approximately 1 h for intact 225 IgG1 to 10 min for 225 Fab, and also fewer antibody species were internalized in case of 225 Fab (*63*). In addition to the greater cell-surface affinity, the bivalent binding and subsequent receptor cross-linking may have altered receptor trafficking in a way that differed from monovalently bound receptors. In the same study (*63*), after saturation binding to the surface of A431 cells was achieved, the percentage of internalized 225 Fab fragments (5%) was approximately 6-fold lower than bivalent IgG1. The catabolism and downregulation of the receptors may increase for a bivalent antibody cross-linking two receptors versus a monovalent antibody species bound to only one receptor, because of the larger size (microbelike) and greater interaction with the cell surface by the bivalent antibody. A recent study by Yarden and co-workers (*67*) directly correlated efficiency of anti-EGFR antibodies in inhibiting tumorigenic cell growth with the size of the antibody−receptor lattices produced at the cell surface, which defined the rate of endocytic clearance and signal blockage (*67*). They found that combining two antibodies that synergistically engage distinct epitopes of the same receptor significantly accelerated EGFR downregulation as compared to a single antibody (*67*). This trend, extrapolated to our case of a monovalent binding Fab, can explain a lower potency of the monovalent species compared with bivalent intact IgG. In the absence of ligand or anti-EGFR, EGFRs undergo metabolic turnover with a half-life of approximately 10−14 h in epithelial cells and 20−48 h in A4321 and other transformed cells (*68*). An average EGFR will internalize and then recycle back to the cell surface dozens of times during its life span, with a low probability of lysosomal degradation and maintaining a steady receptor surface density (*68*). When cells were treated with three different anti-EGFRs in three different experiments, the surface EGFRs were rapidly downregulated, in two cases down to 20% of their original abundance in 1 h (*67*).

In this paper, the monovalent binding affinities of the two anti-EGFR molecules were compared by an SE-HPLC competitive binding assay. The experiment showed that IgG2 has an affinity approximately 5-fold greater than IgG1. This finding was in agreement with the affinity strength determined by surface plasmon resonance (BIACore) and enzyme-linked immunosorbent assay (ELISA) measurements in two separate studies for the IgG2 (ABX-EGF, panitumumab, K_d = 0.05 nM) (*46*) and IgG1 (C225, cetuximab, K_d = 0.1−0.2 nM) (*48*). The agreement between BIACore, ELISA, and SE-HPLC competitive binding was rather expected, because all three methods measured the strength of monovalent affinity. Furthermore, the study showed that binding of one antibody sterically prevented the other antibody from binding to the same soluble EGFR molecule (Figures 10 and 11). This finding was in agreement with the previously published crystallography and other studies with cetuximab (*49*) and panitumumab (*47*), suggesting that both of them interact with the same domain III of soluble EGFR. Our studies confirmed

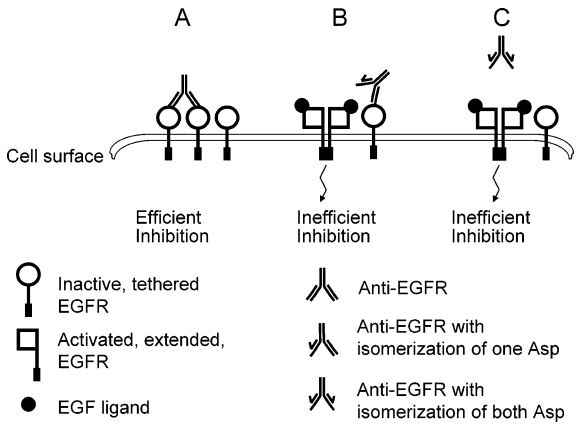

FIGURE 11: Suggested model for the inhibition of cell proliferation by the anti-EGFR IgG2 antibody by use of 32D cell line, which was modified to express the full-length human EGFR. (A) A native anti-EGFR strongly binds two EGFRs on cell surface and disrupts the EGF ligand-induced activation and dimerization of EGFR. The strong binding of anti-EGFR reduced cell proliferation as measured by the relative fluorescence measurements described under Materials and Methods. (B, C) Anti-EGFR antibodies with isoAsp-92 in one or both Fab regions do not bind effectively to disrupt the dimerization and signal transduction and do not suppress the cell proliferation. The model indicated that the anti-EGFR IgG2 antibody behaved as a high-avidity antibody during this assay.

the previous findings (*49*, *47*) in the direct competitive binding experiment.

The in vitro potency of the two anti-EGFR molecules was assessed side-by-side by the cell proliferation assay in a 32D cell line modified to express the full-length human EGFR. This assay showed an approximately 5-fold greater inhibitory effect of IgG2 with respect to IgG1. Although IgG2 was a stronger monovalent binder, the cell proliferation result was not necessarily anticipated, because the avidity-driven mechanism of antibody inhibition of cell proliferation is a very complex process. An increasing body of evidence indicates that the inhibition of proliferation by anti-EGFR antibodies is mediated not only by blocking the ligand binding but also by the accelerated receptor internalization and its endosomal degradation (*47*, *62*, *63*, *67*, *69*). The fact that the difference in inhibition of cell proliferation directly correlated with the strength of the monovalent binding suggests that both antibodies have in general a similar mechanism of inhibition but with a different rate directly related to the monovalent affinity. This hypothesis is supported by the following similarities in the properties of the two monoclonal antibodies. First, they bind to the same domain of EGFR, according to previous reports (*47*, *49*) and in agreement with the SE-HPLC assay results presented here. In addition, previous investigations of IgG1 (*62*, *63*) and this study of IgG1 and IgG2 showed that monovalent species were not effective in inhibiting cell proliferation. Two independent studies (*63*, *69*) using 225 IgG1 and panitumumab IgG2, respectively, reported a general similarity in kinetics of internalization by A431 cells, but the rate was difficult to compare due to some differences in experimental conditions. When these similarities in the general mechanism of action are taken into account, it can be assumed that the higher monovalent affinity of IgG2 led to greater surface residence time of this antibody and/or better cross-linking of receptors. This caused more rapid internalization and downregulation of EGFRs, which led to stronger inhibition of cell proliferation by IgG2. Following this logic, we speculate that the monovalent IgG2 with one isomerized Asp-92 was not efficient in the inhibition of cell proliferation, probably due to a shorter surface residence time (analogous to 225 Fab versus 225 in ref *63*), no cross-linking of receptors, a low rate of internalization (analogous to 225 Fab in ref *63*), and a low rate of downregulation of EGFR. Although our experiments did not directly address the antibody-induced EGFR internalization and trafficking, these experiments along with the hypothesis for the mechanism of inhibition presented above corroborate with previous studies (*62*). A simplified schematic of inhibition of cell proliferation by the bivalent and monovalent species of IgG2 is shown in Figure 11.

ACKNOWLEDGMENT

We acknowledge Ling Cai and Qiang Xiao for producing and purifying the soluble human EGF receptor used in this study. We thank Steve Brych for assistance in accessing and processing crystal structure of antibodies from PDB; Himanshu Gadgil for his contribution to the development of the SE-RP-HPLC/MS method; and Ian Foltz, Chris Vezina, Andrew Kosky, Margaret Ricci, Dan Freeman, Robert Radinsky, Jilin Sun, Tom Boone, Michael Treuheit, and Susan Hershenson for fruitful discussions.

REFERENCES

1. Carpenter, G. (2000) The EGF receptor: a nexus for trafficking and signaling, *Bioassays 22*, 697−707.
2. Heisermann, G. J., and Gill, G. N. (1988) Epidermal growth factor receptor threonine and serine residues phosphorylated in vivo, *J. Biol. Chem. 263*, 13152−13158.
3. Wu, D. G., Wang, L. H., Chi, Y., Sato, G. H., and Sato, J. D. (1990) Human epidermal growth factor receptor residue covalently cross-linked to epidermal growth factor, *Proc. Natl. Acad. Sci. U.S.A. 87*, 3151−3155.
4. Burgess, A. W., Cho, H. S., Eigenbrot, C., Ferguson, K. M., Garrett, T. P. J., Leahy, D. J., Lemmon, M. A., Sliwkowski, M. X., Ward, C. W., and Yokoyama, S. (2003) An Open-and-Shut Case? Recent Insights into the Activation of EGF/ErbB Receptors, *Mol. Cell 12*, 541−552.
5. Yarden, Y., and Sliwkowski, M. X. (2001) Untangling the ErbB signaling network, *Nat. Rev. Mol. Cell Biol. 2*, 127−137.
6. Franklin, M. C., Carey, K. D., Vajdos, F. F., Leahy, D. J., de Vos, A. M., and Sliwkowski, M. X. (2004) Insights into ErbB signaling from the structure of the ErbB2−pertuzumab complex, *Cancer Cell 5*, 317−328.
7. Dawson, J. P., Berger, M. B., Lin, C. C., Schlessinger, J., Lemmon, M. A., and Ferguson, K. M. (2005) Epidermal growth factor receptor dimerization and activation require ligand-induced conformational changes in the dimer interface, *Mol. Cell. Biol. 25*, 7734−7742.
8. Hynes, N. E., and Lane, H. A. (2005) ERBB receptors and cancer: the complexity of targeted inhibitors, *Nat. Rev. Cancer 5*, 341−354.
9. Herbst, R. S., and Shin, D. M. (2002) Monoclonal antibodies to target epidermal growth factor receptor-positive tumors: a new paradigm for cancer therapy, *Cancer 94*, 1593−1611.
10. Kawamoto, T., Sato, J. D., LE, A., Polikoff, J., Sato, G. H., and Mendelsohn, J. (1983) Growth stimulation of a-431 cells by epidermal growth factor identification of high affinity receptors for epidermal growth factor by an anti receptor monoclonal antibody, *Proc. Natl. Acad. Sci. U.S.A. 80*, 1337−1341.
11. Foon, K. A., Yang, X. D., Weiner, L. M., Belldegrun, A. S., Figlin, R. A., Crawford, J., Rowinsky, E. K., Dutcher, J. P., Vogelzang, N. J., Gollub, J., Thompson, J. A., Schwartz, G., Bukowski, R. M., Roskos, L. K., and Schwab, G. M. (2004) Preclinical and clinical evaluations of ABX-EGF, a fully human anti-epidermal growth factor receptor antibody, *Int. J. Radiat. Oncol. Biol. Phys. 58*, 984−990.
12. Scott, A. M., Lee, F. T., Tebbutt, N., Herbertson, R., Gill, S. S., Liu, Z., Skrinos, E., Murone, C., Saunder, T. H., Chappell, B.,

Papenfuss, A. T., Poon, A. M., Hopkins, W., Smyth, F. E., MacGregor, D., Cher, L. M., Jungbluth, A. A., Brechbiel, M. W., Murphy, R., Burgess, A. W., Hoffman, E. W., Johns, T. G., and Old, L. J. (2007) A phase I clinical trial with monoclonal antibody ch806 targeting transitional state and mutant epidermal growth factor receptors, *Proc. Natl. Acad. Sci. U.S.A. 104*, 4071−4076.

13. Adams, G. P., Tai, M. S., McCartney, J. E., Marks, J. D., Stafford, W. F., III, Houston, L. L., Huston, J. S., and Weiner, L. M. (2006) Avidity-mediated enhancement of in vivo tumor targeting by single-chain Fv dimers, *Clin. Cancer Res. 12*, 1599−1605.
14. Gan, H. K., Walker, F., Burgess, A. W., Rigopoulos, A., Scott, A. M., and Johns, T. G. (2007) The epidermal growth factor receptor (EGFR) tyrosine kinase inhibitor AG1478 increases the formation of inactive untethered EGFR dimers. Implications for combination therapy with monoclonal antibody 806, *J. Biol. Chem. 282*, 2840−2850.
15. Geiger, T., and Clarke, S. (1987) Deamidation, isomerization, and racemization at asparaginyl and aspartyl residues in peptides. Succinimide-linked reactions that contribute to protein degradation, *J. Biol. Chem. 262*, 785−794.
16. Oliyai, C., and Borchardt, R. T. (1994) in *Formulation and delivery for proteins and peptides* (Cleland, J. L., and Langer, R., Eds.) pp 47−58, American Chemical Society, Washington, DC.
17. Oliyai, C., and Borchardt, R. T. (1993) Chemical pathways of peptide degradation. IV. Pathways, kinetics, and mechanism of degradation of an aspartyl residue in a model hexapeptide, *Pharm. Res. 10*, 95−102.
18. Oliyai, C., and Borchardt, R. T. (1994) Chemical pathways of peptide degradation. VI. Effect of the primary sequence on the pathways of degradation of aspartyl residues in model hexapeptides, *Pharm. Res. 11*, 751−758.
19. Johnson, B. A., Shirokawa, J. M., Hancock, W. S., Spellman, M. W., Basa, L. J., and Aswad, D. W. (1989) Formation of isoaspartate at two distinct sites during in vitro aging of human growth hormone, *J. Biol. Chem. 264*, 14262−14271.
20. Potter, S. M., Henzel, W. J., and Aswad, D. W. (1993) In vitro aging of calmodulin generates isoaspartate at multiple Asn-Gly and Asp-Gly sites in calcium-binding domains II, III, and IV, *Protein Sci. 2*, 1648−1663.
21. Herman, A. C., Boone, T. C., and Lu, H. S. (1996) in *Formulation, characterization, and stability of protein drugs. Case histories* (Pearlman, R., and Wang, Y. J., Eds.) pp 303−328, Plenum Press, New York.
22. Lam, X. M., Yang, J. Y., and Cleland, J. L. (1997) Antioxidants for prevention of methionine oxidation in recombinant monoclonal antibody HER2, *J. Pharm. Sci. 86*, 1250−1255.
23. Stephenson, R. C., and Clarke, S. (1989) Succinimide formation from aspartyl and asparaginyl peptides as a model for the spontaneous degradation of proteins, *J. Biol. Chem. 264*, 6164−6170.
24. Brennan, T. V., and Clarke, S. (1995) Effect of adjacent histidine and cysteine residues on the spontaneous degradation of asparaginyl- and aspartyl-containing peptides, *Int. J. Pept. Protein Res. 45*, 547−553.
25. Aswad, D. W., Paranandi, M. V., and Schurter, B. T. (2000) Isoaspartate in peptides and proteins: formation, significance, and analysis, *J. Pharm. Biomed. Anal. 21*, 1129−1136.
26. Clarke, S. (1987) Propensity for spontaneous succinimide formation from aspartyl and asparaginyl residues in cellular proteins, *Int. J. Pept. Protein Res. 30*, 808−821.
27. Cleland, J. L., Lam, X. M., Kendrick, B., Yang, J., Yang, T. H., Overcashier, D., Brooks, D., Hsu, C., and Carpenter, J. F. (2001) A specific molar ratio of stabilizer to protein is required for storage stability of a lyophilized monoclonal antibody, *J. Pharm. Sci. 90*, 310−321.
28. Radkiewicz, J. L., Zipse, H., Clarke, S., and Houk, K. N. (2001) Neighboring side chain effects on asparaginyl and aspartyl degradation: an ab initio study of the relationship between peptide conformation and backbone NH acidity, *J. Am. Chem. Soc. 123*, 3499−3506.
29. Capasso, S., and Di Cerbo, P. (2000) Kinetic and thermodynamic control of the relative yield of the deamidation of asparagine and isomerization of aspartic acid residues, *J. Pept. Res. 56*, 382−387.
30. Xiao, G., Bondarenko, P. V., Jacob, J., Chu, G. C., and Chelius, D. (2007) (18)O Labeling method for identification and quantification of succinimide in proteins, *Anal. Chem. 79*, 2714−2721.
31. Cacia, J., Keck, R., Presta, L. G., and Frenz, J. (1996) Isomerization of an aspartic acid residue in the complementarity-determining regions of a recombinant antibody to human IgE: identification and effect on binding affinity, *Biochemistry 35*, 1897−1903.
32. Harris, R. J., Kabakoff, B., Macchi, F. D., Shen, F. J., Kwong, M. Y., Andya, J. D., Shire, S. J., Bjork, N., Totpal, K., and Chen, A. B. (2001) Identification of multiple sources of charge heterogeneity in a recombinant antibody, *J. Chromatogr. B: Biomed. Sci. Appl. 752*, 233−245.
33. Wakankar, A. A., Liu, J., Vandervelde, D., Wang, Y. J., Shire, S. J., and Borchardt, R. T. (2007) The effect of cosolutes on the isomerization of aspartic acid residues and conformational stability in a monoclonal antibody, *J. Pept. Sci. 96*, 1708−1718.
34. Wakankar, A. A., Borchardt, R. T., Eigenbrot, C., Shia, S., Wang, Y. J., Shire, S. J., and Liu, J. L. (2007) Aspartate Isomerization in the Complementarity-Determining Regions of Two Closely Related Monoclonal Antibodies, *Biochemistry 46*, 1534−1544.
35. Di Donato, A., Ciardiello, M. A., de Nigris, M., Piccoli, R., Mazzarella, L., and D'Alessio, G. (1993) Selective deamidation of ribonuclease A. Isolation and characterization of the resulting isoaspartyl and aspartyl derivatives, *J. Biol. Chem. 268*, 4745−4751.
36. Zhang, W., Czupryn, J. M., Boyle, P. T., Jr., and Amari, J. (2002) Characterization of asparagine deamidation and aspartate isomerization in recombinant human interleukin-11, *Pharm. Res. 19*, 1223−1231.
37. Sadakane, Y., Yamazaki, T., Nakagomi, K., Akizawa, T., Fujii, N., Tanimura, T., Kaneda, M., and Hatanaka, Y. (2003) Quantification of the isomerization of Asp residue in recombinant human alpha A-crystallin by reversed-phase HPLC, *J. Pharm. Biomed. Anal. 30*, 1825−1833.
38. Bongers, J., Cummings, J. J., Ebert, M. B., Federici, M. M., Gledhill, L., Gulati, D., Hilliard, G. M., Jones, B. H., Lee, K. R., Mozdzanowski, J., Naimoli, M., and Burman, S. (2000) Validation of a peptide mapping method for a therapeutic monoclonal antibody: what could we possibly learn about a method we have run 100 times?, *J. Pharm. Biomed. Anal. 21*, 1099−1128.
39. Chelius, D., Rehder, D. S., and Bondarenko, P. V. (2005) Identification and characterization of deamidation sites in the conserved regions of human immunoglobulin gamma antibodies, *Anal. Chem. 77*, 6004−6011.
40. Rehder, D. S., Dillon, T. M., Pipes, G. D., and Bondarenko, P. V. (2006) Reversed-phase LC/MS analysis of reduced monoclonal antibodies in pharmaceutics, *J. Chromatogr. A 1102*, 164−175.
41. Ahrer, K., Buchacher, A., Iberer, G., Josic, D., and Jungbauer, A. (2003) Analysis of aggregates of human immunoglobulin G using size-exclusion chromatography, static and dynamic light scattering, *J. Chromatogr. A 1009*, 89−96.
42. Gabrielson, J. P., Brader, M. L., Pekar, A. H., Mathis, K. B., Winter, G., Carpenter, J. F., and Randolph, T. W. (2007) Quantitation of aggregate levels in a recombinant humanized monoclonal antibody formulation by size-exclusion chromatography, asymmetrical flow field flow fractionation, and sedimentation velocity, *J. Pharm. Sci. 96*, 268−279.
43. Sanny, C. G. (2002) Antibody-antigen binding study using size-exclusion liquid chromatography, *J. Chromatogr. B 768*, 75−80.
44. Qian, R. L., Mhatre, R., and Krull, I. S. (1997) Characterization of antigen−antibody complexes by size-exclusion chromatography coupled with low-angle light-scattering photometry and viscometry, *J. Chromatogr. A 787*, 101−109.
45. Santora, L. C., Kaymakcalan, Z., Sakorafas, P., Krull, I. S., and Grant, K. (2001) Characterization of noncovalent complexes of recombinant human monoclonal antibody and antigen using cation exchange, size exclusion chromatography, and BIAcore, *Anal. Biochem. 299*, 119−129.
46. Yang, X. D., Jia, X. C., Corvalan, J. R., Wang, P., Davis, C. G., and Jakobovits, A. (1999) Eradication of established tumors by a fully human monoclonal antibody to the epidermal growth factor receptor without concomitant chemotherapy, *Cancer Res. 59*, 1236−1243.
47. Jakobovits, A., Amado, R. G., Yang, X., Roskos, L., and Schwab, G. (2007) From XenoMouse technology to panitumumab, the first fully human antibody product from transgenic mice, *Nat. Biotechnol. 25*, 1134−1143.
48. Goldstein, N. I., Prewett, M., Zuklys, K., Rockwell, P., and Mendelsohn, J. (1995) Biological efficacy of a chimeric antibody to the epidermal growth factor receptor in a human tumor xenograft model, *Clin. Cancer Res. 1*, 1311−1318.

49. Li, S., Schmitz, K. R., Jeffrey, P. D., Wiltzius, J. J., Kussie, P., and Ferguson, K. M. (2005) Structural basis for inhibition of the epidermal growth factor receptor by cetuximab, *Cancer Cell 7*, 301−311.
50. Harding, J., and Burtness, B. (2005) Cetuximab: an epidermal growth factor receptor chimeric human-murine monoclonal antibody, *Drugs Today 41*, 107−127.
51. Dillon, T. M., Bondarenko, P. V., Rehder, D. S., Pipes, G. D., Kleemann, G. R., and Ricci, M. S. (2006) Optimization of a reversed-phase LC/MS method for characterizing recombinant antibody heterogeneity and stability, *J. Chromatogr. A 1120*, 112−120.
52. Gadgil, H. S., Pipes, G. D., Dillon, T. M., Treuheit, M. J., and Bondarenko, P. V. (2006) Improving mass accuracy of high performance liquid chromatography/electrospray ionization time-of-flight mass spectrometry of monoclonal antibodies, *J. Am. Soc. Mass Spectrom. 17*, 867−872.
53. Zhang, Z. (2004) Prediction of Low-Energy Collision-Induced Dissociation Spectra of Peptides, *Anal. Chem. 76*, 3908−3922.
54. Gadgil, H. S., Bondarenko, P. V., Pipes, G. D., Dillon, T. M., Rehder, D. S., Abel, J., and Treuheit, M. J. (2006) Identification of cysteinylation of a free cysteine in Fab region of recombinant monoclonal IgG1 antibody using Lys-C limited proteolysis coupled with LC/MS analysis, *Anal. Biochem. 355*, 165−174.
55. Korman, A. J., Frantz, J. D., Strominger, J. L., and Mulligan, R. C. (1987) Expression of human class II major histocompatibility complex antigens using retrovirus vectors, *Proc. Natl. Acad. Sci. U.S.A. 84*, 2150−2154.
56. Ritz-Timme, S., and Collins, M. J. (2002) Racemization of aspartic acid in human proteins, *Ageing Res. Rev. 1*, 43−59.
57. Chu, G. C., Chelius, D., Xiao, G., Khor, H. K., Coulibaly, S., and Bondarenko, P. V. (2007) Accumulation of succinimide in a recombinant monoclonal antibody in mildly acidic buffers under elevated temperatures, *J. Pharm. Res. 24*, 1145−1156.
58. Cantor, C. R., and Schimmel, P. R. (1980) in *Biophys. Chem. Part II: Techniques for the Study of Biological Structure and Function*, pp 375−379, W. H. Freeman and Co., San Francisco, CA.
59. Pierce, J. H., Ruggiero, M., Fleming, T. P., Di Fiore, P. P., Greenberger, J. S., Varticovski, L., Schlessinger, J., Rovera, G., and Aaronson, S. A. (1988) Signal transduction through the EGF receptor transfected in IL-3-dependent hematopoietic cells, *Science 239*, 628−631.
60. Yang, S., Qu, S., Perez-Tores, M., Sawai, A., Rosen, N., Solit, D. B., and Arteaga, C. L. (2006) Association with HSP90 inhibits Cbl-mediated down-regulation of mutant epidermal growth factor receptors, *Cancer Res. 66*, 6990−6997.
61. Chen, Y. R., Fu, Y. N., Lin, C. H., Yang, S. T., Hu, S. F., Chen, Y. T., Tsai, S. F., and Huang, S. F. (2006) Distinctive activation patterns in constitutively active and gefitinib-sensitive EGFR mutants, *Oncogene 25*, 1205−1215.
62. Fan, Z., Masui, H., Altas, I., and Mendelsohn, J. (1993) Blockade of epidermal growth factor receptor function by bivalent and monovalent fragments of 225 anti-epidermal growth factor receptor monoclonal antibodies, *Cancer Res. 53*, 4322−4328.
63. Fan, Z., Lu, Y., Wu, X., and Mendelsohn, J. (1994) Antibody-induced epidermal growth factor receptor dimerization mediates inhibition of autocrine proliferation of A431 squamous carcinoma cells, *J. Biol. Chem. 269*, 27595−27602.
64. Parham, P. (1983) On the fragmentation of monoclonal IgG1, IgG2a, and IgG2b from BALB/c mice, *J. Immunol. 131*, 2895−2902.
65. Demignot, S., Garnett, M. C., and Baldwin, R. W. (1989) Mouse IgG2b monoclonal antibody fragmentation. Preparation and purification of Fab, Fc and Fab/c fragments, *J. Immunol. Methods 121*, 209−217.
66. Honegger, A., and Pluckthun, A. (2001) Yet another numbering scheme for immunoglobulin variable domains: an automatic modeling and analysis tool, *J. Mol. Biol. 309*, 657−670.
67. Friedman, L. M., Rinon, A., Schechter, B., Lyass, L., Lavi, S., Bacus, S. S., Sela, M., and Yarden, Y. (2005) Synergistic down-regulation of receptor tyrosine kinases by combinations of mAbs: implications for cancer immunotherapy, *Proc. Natl. Acad. Sci. U.S.A. 102*, 1915−1920.
68. Wiley, H. S. (2003) Trafficking of the ErbB receptors and its influence on signaling, *Exp. Cell Res. 284*, 78−88.
69. Foltz, I. N., King, C. T., and Liang, M. (2007) Panitumumab induces internalization of the epidermal growth factor receptor [abstract B43 plus poster], 17th American Association for Cancer Research−National Cancer Institute−European Organization for the Research and Treatment of Cancer (AACR-NCI Disclosure EORTC) International Conference on Molecular Targets and Cancer Therapeutics; Nov 14−18, 2005, Philadelphia, PA; p 136.

BI7018223